Effect of Molecular Hydrogen on Hydrogen Peroxide in Water Radiolysis

Barbara Pastina[†] **and Jay A. LaVerne***[,‡]

National Research Council Board on Radioactive Waste Management, Washington, D.C. 20418, and Radiation Laboratory, University of Notre Dame, Notre Dame, Indiana 46556

Received: June 14, 2001; In Final Form: August 7, 2001

The long-time chemistry occurring in the radiolysis of water with different types of radiation has been examined. Radiolytic processes were probed by determining the influence of added molecular hydrogen on the formation of hydrogen peroxide in the radiolysis of water with γ rays, 2 and 10 MeV protons, and 5 MeV helium ions. Homogeneous model calculations were used to obtain quantitative information about the yields of radicals and molecular products escaping the heavy ion tracks. The results show that the yields of radicals escaping from the tracks of 10 MeV protons is significant, whereas the corresponding yields with 2 MeV protons and 5 MeV alpha particles are much lower. The addition of molecular hydrogen has a negligible effect on the formation or consumption of hydrogen peroxide in the radiolysis of water using heavy ions with a high linear energy transfer rate, LET. This result is contrary to the predictions of a homogeneous model and suggests that the long-time chemistry of water is not well-known or that a homogeneous model cannot be applied to high LET radiation. There is also the possibility that a significant yield of an oxidizing species is produced at high LET.

Introduction

The long-time effects of water radiolysis are important for both fundamental and practical reasons, and yet, almost no basic experimental studies have been performed, especially with incident heavy ions. Most radiation chemistry studies of water use conventional radiation such as high-energy electrons or γ rays and probe the intratrack chemistry of the water decomposition products with pulse radiolysis or selective scavenger techniques.[1−3] This chemistry ranges from the water dissociation following the passage of the radiation to about 1 μs, the time at which the spatially nonhomogeneous distribution of reactive species has relaxed. Monte Carlo modeling techniques are able to correlate well the different product yields and give mechanistic information on the fast physical and chemical processes occurring on this time scale.[4] Models employing the yields from the fast stage of water radiolysis and appropriate chemical reactions are straightforward to develop because the kinetics is homogeneous.[5,6] However, even small errors in the input parameters can lead to incorrect predicted yields after extrapolating to long periods of time. Experimental yields for only a few of the radicals and molecular species escaping the tracks of heavy ions are known, so it is difficult to determine the accuracy of any model of the long-time radiation chemistry of water with heavy ions.[7,8] Selected experiments that examine the chemistry of water radiolysis in the time domain beyond a few microseconds can greatly aid the development of track models for understanding water radiolysis and for application to practical situations.

Within a few milliseconds following the passage of ionizing radiation in water, the main reducing species are H atoms and H_2 and the main oxidizing species are OH radicals and H_2O_2. Most of the track reactions between the sibling radicals are over by 1 μs in high-energy electron radiolysis, and the subsequent reactions are dominated by the interconversion of oxidizing and reducing radicals and the reaction of radicals with molecular products to re-form water. The interesting reaction to be considered in this work is the reaction of OH radicals with H_2. This reaction and its complement (the H atom reaction with H_2O_2) make up a chain reaction for the reformation of water molecules. In this study, the effects of the addition of H_2 on the yields of H_2O_2 are reported for different types of radiation. Chain reactions are difficult to examine because even small amounts of impurities can interfere. The many competing factors make it necessary to perform experiments on the long-time radiolysis of water, especially with heavy ions.

One very important practical application for examining the long-time radiolysis of water is the use of molecular hydrogen dissolved in the cooling water of pressurized water reactors (PWRs) and boiling water reactors (BWRs) to mitigate corrosion. Hydrogen is known to reduce the concentration of oxidizing species such as O_2 and H_2O_2 and lower the electrochemical corrosion potential (ECP) of metals in the reactor's internal components, which is associated with cracking.[9] The beneficial effect of molecular hydrogen has been known for many years,[10] and justification for its use has been based on a mechanism proposed by Allen et al. in 1952.[11] Very little further fundamental research has been performed on the radiolysis of aqueous hydrogen solutions. The influence of molecular hydrogen on the formation of oxygen and hydrogen peroxide has been examined recently in an experimental reactor as a function of the linear energy transfer (LET = stopping power, $-dE/dx$) of the radiation, of the temperature, and in the presence of different impurities.[8,12] Hydrogen overpressure effects on product formation in the recoil radiolysis of LiOH salts have also been examined.[7] Water in a nuclear reactor is exposed to many types of radiation depending on the distance from the core. Much is known about the general effects of LET on water radiolysis, but the specific yields of all of the water decomposition products

* To whom correspondence should be addressed.
[†] National Research Council Board on Radioactive Waste Management.
[‡] University of Notre Dame.

10.1021/jp012245j CCC: $20.00
Published on Web 09/12/2001

TABLE 1: Characteristics of the Radiation Used in This Work[a]

particle	energy (MeV)	integral LET (eV/nm)	range (mg/cm^2)	dose rate (rad/s)
γ ray		0.23	4×10^5	25
$^1H^+$	2	34.8	7.31	20
	10	13.8	119	100
$^4He^{2+}$	5	156	3.56	25

[a] The energy of the particle is the initial energy of the particle in the sample. The integral LET is the LET averaged over the entire range of the particle.

following the fast chemistry is not known for most high LET particles.[13] It has long been observed that continuous irradiation by low LET radiation leads to steady-state concentrations of H_2 and H_2O_2 that are too low to be observable, whereas high LET radiation can produce significant quantities of these products.[2] Furthermore, the transition from nonhomogeneous to homogeneous chemistry takes place over a much longer time scale, if at all, in the track of a heavy ion compared to a high-energy electron track. This transition gives rise to uncertainties in the application of homogeneous kinetic models to heavy ion radiolysis. The experiments reported here were designed to give fundamental information on the long-time reactions in the radiolysis of water and to obtain estimates of the yields of radicals and molecular products escaping heavy ion tracks.

In this work, the influence of added molecular hydrogen on the formation of hydrogen peroxide was examined in the γ radiolysis and the heavy ion radiolysis of water. The heavy ions consisted of protons (2 or 10 MeV) and 5 MeV helium ions (alpha particles). Pure water or dilute hydrogen peroxide solutions were irradiated with various concentrations of dissolved molecular hydrogen. The purpose of these experiments is to enhance the existing knowledge on the escape yields of radicals with high LET radiation and to examine the effects of molecular hydrogen on the ultimate concentrations of hydrogen peroxide. A homogeneous model calculation was used to predict product concentrations in the long-time radiolysis of water with various amounts of additives. This model is also used to estimate radical and molecular product yields escaping the tracks of heavy ions.

Experimental Section

The heavy ion radiolysis experiments were performed using the facilities of the Nuclear Structure Laboratory of the University of Notre Dame Physics Department. Protons and ^{4}He ions were produced and accelerated using a 10 MeV FN Tandem Van de Graaff. The window assembly and the irradiation procedure were the same as reported earlier.[14,15] After acceleration, the ions were energy and charge-state selected magnetically and the energies of the particles are known with a precision of about 10 kV. Energy loss of the particles in passing through all windows was determined from a standard stopping power compilation.[16] The characteristics of the particles used in this experiment are given in Table 1. The solutions were irradiated with completely stripped particles at a beam current of about 2 nA of charge into 20 mL samples, which were vigorously stirred. Absolute dosimetry was obtained from the product of the integrated beam current and the particle energy. The ranges of the heavy ions (Table 1) are smaller than the sample thickness, so the ions are completely stopped in the solution. The radiation chemical yields represent all processes from the initial particle energy to zero and are therefore track averaged yields.

Radiolysis with γ rays was performed using a Gammacell-220 ^{60}Co source at the Radiation Laboratory of the University of Notre Dame. The dose rate was 1.5 krad/min (15 Gy/min) as determined using the Fricke dosimeter.[17]

The solutions were prepared using water from a Millipore Milli-Q UV system. Degassed solutions were saturated with ultrahigh purity N_2 or Ar. No difference in yields was observed between saturated solutions of Ar and N_2, probably because relatively low doses were used and N_2 was not converted to acid in any significant quantity. Selected mixtures of H_2 were prepared by saturating the solution with pure H_2 or with mixtures of 10 or 1% H_2 in Ar to give solutions of 800, 80, and 8 μM, respectively. Some of the experiments are performed with an initial H_2O_2 concentration of 50 μM in order to examine its disappearance because of reactions with radical species. The pH of the solutions was near neutral (pH $\approx$ 6.5). The hydrogen peroxide concentrations were measured using the iodide method of Ghormley.[17−19] The absorbance of the solution was measured at 350 nm using a diode array spectrophotometer (Hewlett-Packard HP8453). The molar extinction coefficient for the I_3^- was measured at 350 nm with a commercial solution of H_2O_2 (Fischer Scientific). It was found that $\epsilon_{350} = 25\ 850\ M^{-1}\ cm^{-1}$, in good agreement with previous data.[17,19]

Results and Discussion

The passage of ionizing radiation in water leads to a number of ionic and excited states that further decompose to give radical and molecular species. Within a few picoseconds of the initial energy deposition event, the water decomposition products e_{aq}^-, H, OH, and H_2 can be found in clusters along the particle path.[1−3] The initial geometry of the nonhomogeneous spatial distributions of water decomposition products is dependent on the physics of the energy deposition by the incident particle, but it is currently believed that the initial yields are independent of particle type.[13] Track chemistry is defined here as the fast reactions occurring while the nonhomogeneous distributions relax. Because the distributions of reactive species are nonhomogeneous, kinetic models for the track chemistry must include diffusion. In principle, all permutations of reactions of the initial species can occur, but in practice, only 10 or so of the fastest reactions are needed to account for the observed yields.[20] Relaxation of the track occurs within a few microseconds for high-energy electrons, but it can extend to longer times for high LET heavy ions. Secondary reactions involving radicals and product molecules become important as well as acid−base equilibrium reactions at the longer times.[5,6] The complex interactions of radicals and molecular products are difficult to predict, and homogeneous kinetic models are very useful for examining the chemical events occurring in constant radiation fields at long times.

Homogeneous Kinetic Model. Although the short time radiation chemistry ($<1\ \mu$s) of water can be described with only a few equations, examination of the long-time kinetics requires the contributions of many more reactions. The complex interaction of radical species as they interconvert and react with molecular products is very difficult to follow without the aid of kinetic models. The model chosen for this work is essentially the same as previously developed by Elliot and McCracken, and the appropriate reactions are listed in Table 2.[5] Basically, the yields of water decomposition products following the end of the nonhomogeneous phase, called the escape yields, are allowed to react homogeneously according to the set of reactions given in Table 2. During the irradiation period, water decomposition products were formed continuously in conjunction with

TABLE 2: Reactions and Rate Constants Used in the Model Calculations

	Formation Reaction			
1	H_2O	→	e^-_{aq}, H, OH, H_2, H_2O_2, HO_2	
	Equilibria			pK_a
2	H_2O	↔	$H^+ + OH^-$	13.999
3	H_2O_2	↔	$H^+ + HO_2^-$	11.65
4	OH	↔	$H^+ + O^-$	11.9
5	HO_2	↔	$H^+ + O_2^-$	4.57
6	H	↔	$H^+ + e^-_{aq}$	9.77
	Acid − Base Reactions			Rate coefficients ($M^{-1}s^{-1}$ or s^{-1})
7	$H^+ + OH^-$	→	H_2O	1.4×10^{11}
8	H_2O	→	$H^+ + OH^-$	$k_7 \times K_2/[H_2O]$
9	H_2O_2	→	$H^+ + HO_2^-$	$k_{10} \times K_3$
10	$H^+ + HO_2^-$	→	H_2O_2	5.0×10^{10}
11	$H_2O_2 + OH^-$	→	$HO_2^- + H_2O$	1.3×10^{10}
12	$HO_2^- + H_2O$	→	$H_2O_2 + OH^-$	$k_{11} \times K_2/ K_3 \times [H_2O]$
13	$e^-_{aq} + H_2O$	→	$H + OH^-$	1.9×10^{1}
14	$H + OH^-$	→	$e^-_{aq} + H_2O$	2.2×10^{7}
15	H	→	$e^-_{aq} + H^+$	$k_{16} \times K_6$
16	$e^-_{aq} + H^+$	→	H	2.3×10^{10}
17	$OH + OH^-$	→	$O^- + H_2O$	1.3×10^{10}
18	$O^- + H_2O$	→	$OH + OH^-$	$k_{17} \times K_2/ K_4 \times [H_2O]$
19	OH	→	$O^- + H^+$	$k_{20} \times K_4$
20	$O^- + H^+$	→	OH	1.0×10^{11}
21	HO_2	→	$O_2^- + H^+$	$k_{22} \times K_5$
22	$O_2^- + H^+$	→	HO_2	5.0×10^{10}
23	$HO_2 + OH^-$	→	$O_2^- + H_2O$	5.0×10^{10}
24	$O_2^- + H_2O$	→	$HO_2 + OH^-$	$k_{23} \times K_2/ K_5 \times [H_2O]$
	Chemical Reactions			
25	$e^-_{aq} + OH$	→	OH^-	3.0×10^{10}
26	$e^-_{aq} + H_2O_2$	→	$OH + OH^-$	1.1×10^{10}
27	$e^-_{aq} + O_2^- + H_2O$	→	$HO_2^- + OH^-$	$1.3 \times 10^{10}/[H_2O]$
28	$e^-_{aq} + HO_2$	→	HO_2^-	2.0×10^{10}
29	$e^-_{aq} + O_2$	→	O_2^-	1.9×10^{10}
30	$e^-_{aq} + e^-_{aq} + 2H_2O$	→	$H_2 + 2OH^-$	$5.5 \times 10^{9}/[H_2O]$
31	$e^-_{aq} + H + H_2O$	→	$H_2 + OH^-$	$2.5 \times 10^{10}/[H_2O]$
32	$e^-_{aq} + HO_2^-$	→	$O^- + OH^-$	3.5×10^{9}
33	$e^-_{aq} + O^- + H_2O$	→	$OH^- + OH^-$	$2.2 \times 10^{10}/[H_2O]$
34	$e^-_{aq} + O_3^- + H_2O$	→	$O_2 + OH^- + OH^-$	$1.6 \times 10^{10}/[H_2O]$
35	$e^-_{aq} + O_3$	→	O_3^-	3.6×10^{10}
36	$H + H_2O$	→	$H_2 + OH$	1.1×10^{1}
37	$H + O^-$	→	OH^-	1.0×10^{10}
38	$H + HO_2^-$	→	$OH + OH^-$	9.0×10^{7}
39	$H + O_3^-$	→	$OH^- + O_2$	1.0×10^{10}
40	H + H	→	H_2	7.8×10^{9}
41	H + OH	→	H_2O	7.0×10^{9}
42	$H + H_2O_2$	→	$OH + H_2O$	9.0×10^{7}
43	$H + O_2$	→	HO_2	2.1×10^{10}
44	$H + HO_2$	→	H_2O_2	1.8×10^{10}
45	$H + O_2^-$	→	HO_2^-	1.8×10^{10}
46	$H + O_3$	→	HO_3	3.8×10^{10}
47	OH + OH	→	H_2O_2	3.6×10^{9}
48	$OH + HO_2$	→	$H_2O + O_2$	6.0×10^{9}
49	$OH + O_2^-$	→	$OH^- + O_2$	8.2×10^{9}
50	$OH + H_2$	→	$H + H_2O$	4.3×10^{7}
51	$OH + H_2O_2$	→	$HO_2 + H_2O$	2.7×10^{7}
52	$OH + O^-$	→	HO_2-	2.5×10^{10}
53	$OH + HO_2^-$	→	$HO_2 + OH^-$	7.5×10^{9}
54	$OH + O_3^-$	→	$O_3 + OH^-$	2.6×10^{9}
55	$OH + O_3^-$	→	$O_2^- + O_2^- + H^+$	6.0×10^{9}
56	$OH + O_3$	→	$HO_2 + O_2$	1.1×10^{8}
57	$HO_2 + O_2^-$	→	$HO_2^- + O_2$	8.0×10^{7}
58	$HO_2 + HO_2$	→	$H_2O_2 + O_2$	7.0×10^{5}
59	$HO_2 + O^-$	→	$O_2 + OH^-$	6.0×10^{9}
60	$HO_2 + H_2O_2$	→	$OH + O_2 + H_2O$	5.0×10^{-1}
61	$HO_2 + HO_2^-$	→	$OH + O_2 + OH^-$	5.0×10^{-1}
62	$HO_2 + O_3^-$	→	$O_2 + O_2 + OH^-$	6.0×10^{9}
63	$HO_2 + O_3$	→	$HO_3 + O_2$	5.0×10^{8}
64	$O_2^- + O_2^- + 2H_2O$	→	$H_2O_2 + O_2 + 2OH^-$	$1.0 \times 10^{2}/2[H_2O]$
65	$O_2^- + O^- + H_2O$	→	$O_2 + 2OH^-$	$6.0 \times 10^{8}/[H_2O]$
66	$O_2^- + H_2O_2$	→	$OH + O_2 + OH^-$	1.3×10^{-1}

TABLE 2: (Continued)

	Chemical Reactions			
67	$O_2^- + HO_2^-$	→	$O^- + O_2 + OH^-$	1.3×10^{-1}
68	$O_2^- + O_3^- + H_2O$	→	$O_2 + O_2 + 2OH^-$	$1.0 \times 10^4/[H_2O]$
69	$O_2^- + O_3$	→	$O_3^- + O_2$	1.5×10^9
70	$O^- + O^- + H_2O$	→	$HO_2^- + OH^-$	$1.0 \times 10^9/[H_2O]$
71	$O^- + O_2$	→	O_3^-	3.6×10^9
72	$O^- + H_2$	→	$H + OH^-$	8.0×10^7
73	$O^- + H_2O_2$	→	$O_2^- + H_2O$	5.0×10^8
74	$O^- + HO_2^-$	→	$O_2^- + OH^-$	4.0×10^8
75	$O^- + O_3^-$	→	$O_2^- + O_2^-$	7.0×10^8
76	$O^- + O_3$	→	$O_2^- + O_2$	5.0×10^9
77	O_3^-	→	$O_2 + O^-$	3.3×10^3
78	$O_3^- + H^+$	→	$O_2 + OH$	9.0×10^{10}
79	HO_3	→	$O_2 + OH$	1.1×10^5

TABLE 3: *G* Values Used in Model Calculations (Units of Molecules/100 eV)

species	γ rays	10 MeV H	2 MeV H	5 MeV He
$G(e^-_{aq})$	2.60	0.90	0.30	0.15
$G(H)$	0.66	0.57	0.20	0.10
$G(H_2)$	0.45	0.64	0.90	1.20
$G(OH)$	2.70	1.18	0.63	0.35
$G(H_2O_2)$	0.70	0.74	0.76	1.00
$G(HO_2)$	0.02	0.03	0.05	0.10
$G(H^+)$	3.10	1.10	0.36	0.18
$G(OH^-)$	0.50	0.20	0.06	0.03

their reaction until the desired dose was received by the system. After that time, the production of water decomposition products was terminated, and the reactions were allowed to continue until all radical species were gone. The escape yields are given in Table 3, and the dose rates appropriate to the heavy ion radiolysis of this work are given in Table 1. The dose rate for γ radiolysis was 25 krad/s (1 krad = 10 Gy) as determined by the Fricke dosimeter. The dose rates for heavy ion radiolysis are for the experimental conditions of 2 nA beam currents into 20 mL of water. The rate coefficients used throughout this work are taken from refs 7 and 21−23. There is very little disagreement on the values of most of the rate coefficients because they have been measured independently and used extensively in nonhomogeneous model calculations.[4] The major uncertainties in the rate coefficients are with the very slow reactions and will be discussed below. The simulation of the reactions was performed using the Facsimile code.[24,25]

The predicted results for the γ radiolysis of water are shown in Figure 1. It can be seen that the concentrations of e_{aq}^-, H, OH, H_2O_2, and H_2 initially increase at a constant rate because of the radiolytic source terms (product of escape yields and dose rate). Within a few milliseconds of the start of the irradiation, the e_{aq}^- concentration plateaus at a value below that of the H atom. Conversion of the e_{aq}^- to H atom occurs mainly by reactions 13 and 16. Within about 100 seconds (2500 rad), all products from water radiolysis have reached their limiting values, which are nearly independent of dose rate. It can be seen that the major radicals are OH, H, and the O_2^-/HO_2 conjugate pair, whereas the dominant molecular species are H_2O_2, O_2, and H_2. All concentrations are below 1 μM, which is about the lowest detection limit for most analytical techniques. Therefore, the predicted results agree with the general assessment that there is no net decomposition of water in the γ radiolysis of neat water.

The dominant long-time reactions of the radicals produced in water radiolysis are with molecular species and not with each other. H atoms mainly react with water (reaction 36) up to about 10 s (250 rad) when the O_2 concentration becomes large enough to scavenge them (reaction 43). The e_{aq}^- mainly reacts with H^+ (reaction 16) and with water (reaction 13) up to about 1 s

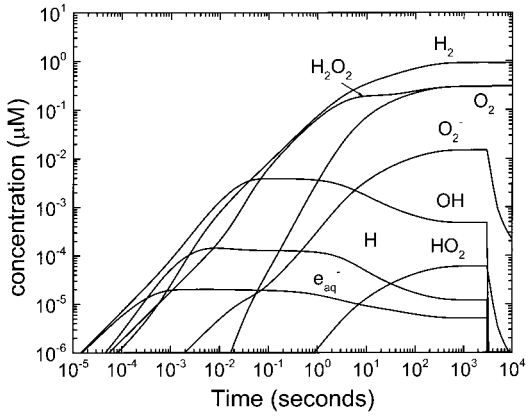

Figure 1. Temporal dependence of water decomposition product concentrations for a 1 h γ radiolysis (25 rad/s) of neat water.

(25 rad), and then the major reactions are with H_2O_2 (reaction 26) and O_2 (reaction 29) as their concentrations rise. The main reaction of OH radicals is with OH^- (reaction 17) at all times, but it does react to some extent at times above 10 s (250 rad) with O_2^- (reaction 49) and H_2 (reaction 50). The major additional formation of H_2O_2 above that escaping from the track is the combination of OH radicals (reaction 47), although this reaction is never the dominant reaction of OH radicals at long times. An additional source of H_2 above that escaping from the track is the reaction of H with water (reaction 36).

The addition of H_2 or H_2O_2 to the solution will lead to significant scavenging of the radical species by these molecules. With sufficient concentrations of H_2 and H_2O_2, there is a net interconversion of OH radicals and H atoms by reactions 42 and 50. The equivalent stoichiometric equation is $H_2 + H_2O_2 = 2H_2O$, resulting in a chain reaction for the net addition of H atoms and OH radicals to re-form water. With a constant source of radicals, this reaction will consume all of the H_2 or H_2O_2, whichever is the lesser. There must be a sufficient supply of radicals to continue the chain propagation, a situation not necessarily found in heavy ion radiolysis. The termination of the chain reaction can be caused by the accumulation of O_2, which scavenges the H atoms (reaction 43). A large excess of hydrogen peroxide can also break the chain reaction because it consumes part of the OH radicals before reaction with H_2 can occur and because it leads to the formation of O_2.

The recombination process for radicals to re-form water is effective when the length of the propagation step in the chain reaction is high, i.e., when the concentration of the radical species is high. Therefore, the chain reaction is the most effective in the presence of low LET radiation, such as γ radiation, because of the high radical yields (H, OH, and e^-_{aq}) and low molecular yields (H_2O_2, H_2, and HO_2). A heavy ion beam, i.e., a high LET radiation, will lead to either a shortening of the

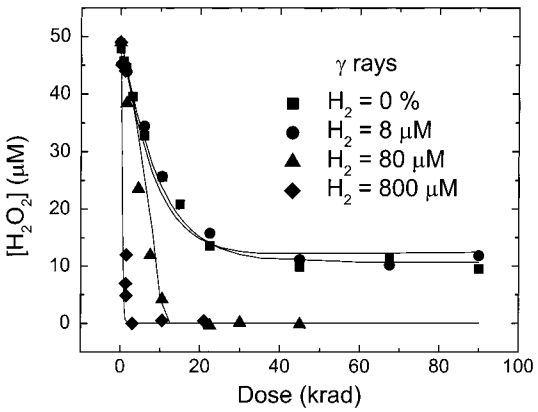

Figure 2. H_2O_2 concentration dependence on dose in the γ radiolysis of aqueous 50 μM H_2O_2 solutions with various concentrations of added molecular hydrogen: (■) no H_2, (●) 8 μM H_2, (▲) 80 μM H_2, (◆) 800 μM H_2. The solid lines are the homogeneous model predictions.

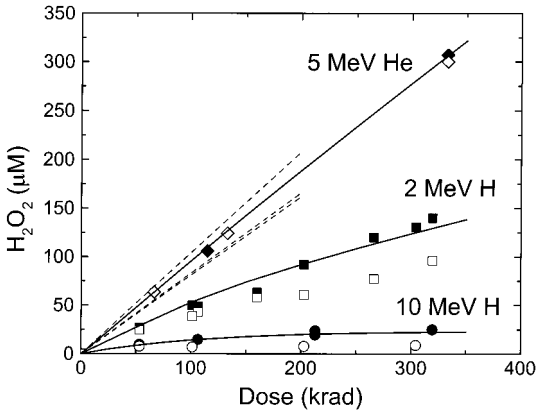

Figure 3. H_2O_2 concentration dependence on dose in the heavy ion radiolysis of water with no H_2 (filled symbols) and H_2 saturated (800 μM; open symbols): (◆) 5 MeV He, (■) 2 MeV H, and (●) 10 MeV H. The solid lines are the homogeneous model predictions for solutions with no H_2, and the dashed lines are the estimated concentrations based on the escape yields (decreasing in the order He, 2 MeV H, and 10 MeV H).

chain process or completely stop it with formation of stable decomposition products from water radiolysis (O_2, H_2O_2, and H_2). It has been shown that water decomposition by radiolysis in the presence of H_2 is a threshold phenomenon as a function of the LET of the radiation.[8,12] With low LET radiation, no stable decomposition products (O_2 and H_2O_2) are detectable. A progressive increase of the LET leads to an increase in the formation of O_2 and H_2O_2 indicating that the chain reaction has stopped or is at least inhibited. The threshold depends on different factors such as the H_2 concentration, the temperature of water, the presence of impurities, and their nature.

***γ* Radiolysis.** The extensive literature on γ radiolysis helps in predicting the long-time radiolysis of water. However, the exact effects of H_2 on H_2O_2 production have not been determined. Mixed pile irradiations showed that the addition of H_2 to solutions of H_2O_2 would decrease the concentration of the latter considerably.[8] A series of γ irradiations were performed in order to directly compare the results with those obtained with heavy ions and to check the predictive ability of the homogeneous model calculations. Figure 2 shows the depletion of H_2O_2 in the γ radiolysis of water in the presence and in the absence of added H_2. Model calculations, see Figure 1, show that the limiting concentration of H_2O_2 in the γ radiolysis of water is below 1 μM, which is below the lowest detectable limit with the experimental techniques used in this work. Therefore, to examine the effect of dissolved H_2 in γ radiolysis it is necessary to add a small amount of initial H_2O_2 (50 μM) so that it can react with the radical species H, OH, and e^-_{aq}. The results in Figure 2 show that there is a net decrease of H_2O_2 in γ radiolysis and more is consumed in the presence of H_2 than in neat water. This result is due to the scavenging of the OH radicals by H_2 and propagation of the chain reaction.

Simulations of the γ radiolysis of water were performed using the homogeneous model with the escape yields given in Table 3. It can be seen that the model can reproduce well the results with and without added H_2. In only the lowest H_2 concentration is the high dose limit of H_2O_2 concentration great enough to be experimentally determined. The limiting values for H_2O_2 with the other two concentrations of H_2 are too low to be measured, so the accuracy of the model in those situations cannot be examined. The model predicts that the initial H_2O_2 concentration would have to be increased by about 2 orders of magnitude before the low limit of H_2O_2 with H_2 saturated solutions can be measured using the present experimental technique. Such a large H_2O_2 concentration will perturb the track chemistry and was not examined.

Heavy Ion Radiolysis of Water. H_2O_2 production was determined in the 5 MeV helium and 10 and 2 MeV proton radiolysis of water. Water saturated with an inert gas, Ar or N_2, and solutions saturated with H_2 were examined. No difference in yields was observed between saturated solutions of Ar and N_2, probably because the doses were too low to convert much of the N_2 to acid. Figure 3 shows the H_2O_2 formation as a function of the absorbed dose in heavy ion radiolysis of water without added H_2O_2. It can be seen that the formation of H_2O_2 increases with increasing LET of the incident particle. The H_2O_2 concentration dependence found with protons is not linear as a function of the absorbed dose, indicating that this product is reacting at long times with radicals produced in the radiolysis. The predicted yields based on the estimated escape yields are shown as the dashed lines in Figure 3. Only in the case of helium ion radiolysis is the observed yield even close to the value predicted from the escape yield. With increasing LET of the heavy ion, the escape yields of radicals decrease. In the 5 MeV helium ion radiolysis of water, the radical yields have dropped sufficiently that decomposition of the H_2O_2 occurs to only a small extent at the longer times.

The results found on the addition of H_2 in the heavy ion radiolysis of water are shown as the open symbols in Figure 3. It can be seen that with increasing LET there is a proportionately less effect of H_2 on the formation of H_2O_2. Virtually no effect on H_2O_2 formation is found in H_2 saturated solutions irradiated with 5 MeV helium ions. This result is in agreement with the predictions of the neat water systems based on the escape yields. At the other extreme, low LET ions such as 10 MeV protons behave much like γ radiolysis, with H_2O_2 showing a large dependence on H_2 concentration.

Heavy ion radiolysis experiments were also performed with added H_2O_2 in order to examine its decomposition due to radicals escaping the track. Figure 4 shows the results for the observed H_2O_2 concentration as a function of dose for solutions initially 50 μM in H_2O_2. The two highest LET particles, 5 MeV helium ions and 2 MeV protons, show increasing H_2O_2 concentrations with increasing dose. For both of these ions, the rate of increase is less than expected from the escape yields, but clearly, the H_2O_2 is being formed at a greater rate than it is being consumed by radical reactions. The 10 MeV proton results show a slight decrease in H_2O_2 concentrations with increasing dose, which more closely resembles that observed with γ

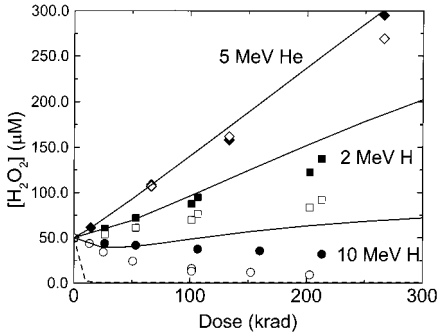

Figure 4. H_2O_2 concentration dependence on dose in the heavy ion radiolysis of 50 μM H_2O_2 solutions with no H_2 (closed symbols) and H_2 saturated (800 μM; open symbols): (◆) 5 MeV He, (■) 2 MeV H, and (●) 10 MeV H. The solid lines are the homogeneous model predictions for solutions with no H_2, and the dashed line is for H_2 saturated helium ion radiolysis.

radiolysis. The relative decrease in H_2O_2 concentrations with increasing dose is much less for 10 MeV protons (36%) than with γ radiolysis (81%). The track average LET with 10 MeV protons is about 14 eV/nm, and sufficient amounts of radicals are escaping the track to lead to a net decrease in H_2O_2 concentration. The track average LET of a 2 MeV proton is only about 35 eV/nm, which is above the threshold where H_2O_2 is formed at a rate greater than it is consumed. The LET at which H_2O_2 production is about the same as consumption is estimated to be about 20 eV/nm, which corresponds to a 5 MeV proton. This is a critical LET, and below it, there are insufficient amounts of radicals escaping the track to carry the propagation step of the chain reaction.

The simulations of the results obtained with heavy ions are shown as the solid lines in Figures 3 and 4. The homogeneous model and the escape yields listed in Table 3 were used. A first estimation of the escape yields was made using radiation chemical yields in the literature and material balance.[5,17,26−30] The escape yields were varied until the predicted results matched the measured values for neat water. Figure 3 shows that a very good agreement to the data is obtained with the escape yields listed in Table 3. For those species that have been measured, the escape yields used here are within a few percent of the values given in the literature. The agreement with those values suggests that the escape yields used in the model calculations well represent the true yields. The predictions of the model are reasonably sensitive to the escape yields chosen, but the use of a deterministic model may be in doubt, see below. Therefore, experiments measuring the escape yield for more ions at different energies are desirable.

Good agreement between the model predictions and experiments is found for the helium ion radiolysis of water with added H_2O_2. However, the agreement is poor for the proton results with aqueous solutions of H_2O_2, especially at the higher doses. The same escape yields for each of the heavy ions was used in the calculations with and without added H_2O_2. The fastest reaction of H_2O_2 is with the hydrated electron, and at 50 μM, the lifetime of this reaction is about 2 μs, which is too long to have a significant effect on the track chemistry. It appears that there is a problem matching the long-time chemistry of protons. The problem could be in the application of a homogeneous model to a system that has a long transition from the track chemistry to the homogeneous phase. It is also possible equilibrium processes that are not accurately described by the homogeneous model are dominating the long-time chemistry of protons. Selective examination of a number of reactions did not reveal any particular one in error. Further experiments and the application of Monte Carlo track codes may lead to a solution to this problem.

The addition of H_2 gives a noticeable decrease in the experimental values for H_2O_2 concentrations at the lowest LET. However, the simulations predict a much larger effect for all of the particles. The dotted line in Figure 4 shows the predicted H_2O_2 dependence for the helium ion radiolysis of solutions saturated with H_2. The observed results are far from the predicted ones. No reason for this discrepancy is known. Previous results using tritium recoil particles showed little effect on H_2O_2 concentrations up to about 3 atm of H_2 overpressure.[7] Those experiments involved the neutron radiolysis of LiOH solutions to give the tritium recoil. The results were interpreted in terms of oxidation/reduction reactions of a metal impurity in the LiOH. No metals are expected in the systems examined here. It is equally unclear how an impurity would affect the heavy ion results and not the γ radiolysis.

Equilibrium conditions, i.e., the long time steady-state concentrations, are reached with doses of about 50 krad in the γ radiolysis of H_2O_2 solutions. On the other hand, hundreds of Mrad of energy are required to reach the steady state limits with the heavy ions. Unfortunately, only the steady-state results at 1% H_2 (8 μM) were examined in γ radiolysis because of the lower limit of detection of H_2O_2. It is possible that several reactions are leading to a coupled equilibrium in which one or more reactions are incorrect in the model. The buildup of an oxidizing species, O_2 for instance, can also give the observed effects. High concentrations of an oxidizing species will scavenge H atoms and terminate the chain reaction. No experimental determination of a large O_2 yield in heavy ion radiolysis has been made, but future experiments will examine this possibility. Of course, the results could be due to an experimental artifact caused by the depletion of the H_2. However, the H_2 effect is occurring in the homogeneous regime and the bulk H_2 adsorbed in the water is not likely to be depleted in the present experimental configuration because H_2 is bubbled through the solution continuously during the irradiation. Decreasing the beam current by over 1 magnitude also had no effect on the observed results. It is also possible that a homogeneous model cannot be used for predicting long-time chemistry with some irradiations because of the overlap with the track chemistry regime. Further detailed Monte Carlo calculations are in progress to examine this possibility. Clearly, the homogeneous model must be used with caution in practical applications involving high LET radiations.

The major reactions that may be causing problems in the model calculations are the slow reactions, especially in the solutions with added H_2. The only reaction of H_2 is with OH radicals (reaction 50). The H atom produced from this reaction is then required to react with H_2O_2 (reaction 42) to propagate the chain. This latter reaction is in competition with H atom reaction with water (reaction 36). The rate coefficient for the later reaction is very low. Its value was obtained by a model fit to a series of reactions and could be in significant error.[31] However, it is not understood why this reaction would cause a problem with the heavy ion radiolysis and not the γ radiolysis. The good results with modeling the γ radiolysis suggests that the kinetics assumed in the model is basically sound.

One of the goals of this work was to provide information on the radiation chemistry that pertains to reactors, which primarily involves neutrons and γ rays. In most reactors, the neutron energy distribution, and the subsequent proton recoils, is lower in energy than the 10 MeV protons examined here. The lowest practical proton energy capable with the present facility is about

2 MeV because of excessive energy straggling at lower energies. Interpolation between the results with 2 and 10 MeV protons can give predictions of the radiation chemistry at other proton energies. However, any realistic application to reactors will involve the use of models, and the results here are ideally suited for model development.

In the presence of a mixed field radiation, such as that in the cooling circuit of a power reactor, the effects of low and high LET radiation are simultaneous. The γ component of the radiation may supply the necessary radical concentrations to carry the chain reaction and destroy the molecular products formed by the high LET component. Under the present conditions, the critical LET corresponding to the threshold of water decomposition appears to be near 20 eV/nm, which corresponds to 5 MeV protons. Below this threshold, essentially all of the products formed by radiolysis, including hydrogen peroxide, are recombined by the radicals through the chain reaction. This chain reaction is accelerated by the dissolved molecular hydrogen. Above this critical LET, the water decomposes to form H_2, H_2O_2, and O_2 because not enough radicals are escaping into the bulk solution. Obviously, the relative fraction of γ ray to high LET radiation in the primary coolant of nuclear reactors, as well as other factors such as temperature and impurities, will determine if water is protected by decomposition under normal reactor operating conditions. In case of an accident or other mishap resulting in a local accumulation of H_2O_2 or O_2, the water reformation would stop even in the presence of γ radiation only. [1] An excess of H_2 will minimize the effects with γ rays but not the high LET radiation component.

Conclusions

A quantitative insight into the effects of the track structure of different heavy ions on the yields of radicals and molecular products from the decomposition of water has been obtained. These experiments involved the radiolysis of a number of aqueous solutions containing various concentrations of added H_2 and H_2O_2. H_2 is an OH radical scavenger and is used to probe the escape yields of radicals in the presence of an initial small concentration of H_2O_2. From the experimental results, it appears that the track structure of 10 MeV protons is somewhat similar to that for γ radiation with a slightly smaller fraction of radicals escaping into the bulk water. Higher LET particles have very low radical escape yields in pure water leading to a net decomposition of bulk water. The threshold for this process is about 20 eV/nm (a 5 MeV proton). The addition of H_2 promotes the recombination of radicals to water for the lowest LET radiation. However, experimentally, no effect due to added H_2 is observed at the highest LET. These results are contradictory to homogeneous model predictions.

Acknowledgment. The authors thank Professor J. J. Kolata for making the facilities of the Notre Dame Nuclear Structure Laboratory available. The latter is funded by the National Science Foundation. The work described herein was supported by Grant DE-FG03-99SF21923 of the Nuclear Energy Research Initiative Program of the U. S. Department of Energy. This contribution is NDRL-4310 from the Notre Dame Radiation Laboratory, which is supported by the Office of Basic Energy Sciences of the U. S. Department of Energy.

References and Notes

(1) Allen, A. O. *The Radiation Chemistry of Water and Aqueous Solutions*; Van Nostrand: New York, 1961.
(2) Draganic, I. G.; Draganic, Z. D. *The Radiation Chemistry of Waters* Academic Press: New York, 1971.
(3) Buxton, G. V. In *Radiation Chemistry: Principles and Applications*; Farhataziz., Rodgers, M. A. J., Eds.; VCH Publishers: New York, 1987; p 321.
(4) Pimblott, S. M.; LaVerne, J. A. *J. Phys. Chem. A* **1997**, *101*, 5828.
(5) Elliot, A. J.; McCracken, D. R. *Fusion Eng. Des.* **1990**, *13*, 21.
(6) Christensen, H. *Nucl. Technol.* **1995**, *109*, 373.
(7) Elliot, A. J.; Chenier, M. P. *J. Nucl. Mater.* **1992**, *187*, 230.
(8) Pastina, B.; Isabey, J.; Hickel, B. *J. Nucl. Mater.* **1999**, *264*, 309.
(9) Cowan, R. L. *Water Chemistry of Nuclear Reactor Systems 7*; British Nuclear Energy Society: London, 1996.
(10) *BWR Water Chemistry Guidelines, 1993 Revision: Normal and Hydrogen Water Chemistry*, Electric Power Research Institute, Report TR-103515, 1994.
(11) Allen, A. O.; Hochanadel, J.; Ghormley, J.; Davis, T. W. *J. Phys. Chem.* **1952**, *56*, 575.
(12) Pastina, B. Ph.D. Thesis, Université Paris-Sud, Paris, France, 1997; no. 4862.
(13) LaVerne, J. A. *Radiat. Res.* **2000**, *153*, 487.
(14) LaVerne, J. A.; Schuler, R. H. *J. Phys. Chem.* **1987**, *91*, 5770.
(15) LaVerne, J. A.; Schuler, R. H. *J. Phys. Chem.* **1987**, *91*, 6560.
(16) Ziegler, J. F.; Biersack, J. P.; Littmark, U. *The Stopping Power and Range of Ions in Solids*; Pergamon: New York, 1985.
(17) Pastina, B.; LaVerne, J. A. *J. Phys. Chem. A* **1999**, *103*, 1592.
(18) Ghormley, J. A.; Stewart, A. C. *J. Am. Chem. Soc.* **1956**, *78*, 2934.
(19) Hochanadel, C. J. *J. Phys. Chem.* **1952**, *56*, 587.
(20) Schwarz, H. A. *J. Phys. Chem.* **1969**, *73*, 1928.
(21) Buxton, G. V.; Greenstock, C. L.; Helman, W. P.; Ross, A. B. *J. Phys. Chem. Ref. Data* **1988**, *17*, 513.
(22) Elliot, A. J.; Buxton, G. V. *J. Chem. Soc., Faraday Trans.* **1992**, *88*, 2465.
(23) Mezyk, S. P.; Bartels, D. M. *J. Chem. Soc., Faraday Trans.* **1995**, *91*, 3127.
(24) Chance, E. M.; Curtis, A. R.; Jones, I. P.; Kirby, C. R. *Report AERE-R 8775*; AERE: Harwell, 1977.
(25) Burns, W. G.; Sims, H. E.; Goodall, J. A. B. *Radiat. Phys. Chem.* **1984**, *23*, 143.
(26) Schwarz, H. A.; Caffrey, J. M.; Scholes, G. *J. Am. Chem. Soc.* **1959**, *81*, 1801.
(27) LaVerne, J. A.; Schuler, R. H.; Burns, W. G. *J. Phys. Chem.* **1986**, *90*, 3238.
(28) LaVerne, J. A. *Radiat. Res.* **1989**, *118*, 201.
(29) LaVerne, J. A.; Yoshida, H. *J. Phys. Chem.* **1993**, *97*, 10720.
(30) LaVerne, J. A.; Pimblott, S. M. *J. Phys. Chem.* A **2000**, *104*, 9820.
(31) Hartig, K. T.; Getoff, N. *J. Photochem.* **1982**, *18*, 29.